RSC Advances

PAPER

View Article Online
View Journal | View Issue

Cite this: *RSC Adv.*, 2017, **7**, 53653

Computational design of enhanced photocatalytic activity of two-dimensional cadmium iodide†

Lin Tao and Le Huang *

Received 31st August 2017
Accepted 1st November 2017

DOI: 10.1039/c7ra09687a

rsc.li/rsc-advances

The recent synthesis of two-dimensional cadmium iodide (CdI_2) opens up the questions of its properties and potential applications in optoelectronic and photovoltaic devices. Using a first-principles design approach, the electronic structure of 2D CdI_2 is determined. The calculated results of the band gaps and band edges demonstrated that CdI_2 is a suitable photocatalyst for water splitting. Monolayer CdI_2 should exhibit a relatively low photocatalytic activity due to its large band gap (about 3.0 eV). Some favourable doping can introduce extra bands to its band gap with the redox potentials of water straddled in its band gap, which can lead to improved photocatalytic performance. Multilayer CdI_2 with a narrower band gap may absorb a finite amount of visible light, making it a more suitable photocatalyst. Furthermore, multilayer CdI_2 exhibits significant modulation of its band gap and band alignment by applying normal strain and a vertical electric field. A reduced band gap with the CBM and VBM approaching the H^+/H_2 and the H_2O/O_2 potentials, respectively, can result in an enhanced photocatalytic activity by applying normal strain and a vertical electric field.

Introduction

The conversion of solar light into hydrogen by photocatalytic water splitting is an attractive technology for producing an alternative energy resource to fossil fuels without environmental pollution.[1–4] To achieve high efficiency, the photocatalyst should satisfy several requirements.[5,6] The photocatalyst should have suitable band edges to straddle the redox potentials of water. Specifically, its conduction band minimum (CBM) should be higher than the hydrogen reduction potential (H^+/H_2) and the valence band maximum (VBM) should be lower than the water oxidation potential (H_2O/O_2). The standard H^+/H_2 and H_2O/O_2 potentials with respect to the vacuum level are −4.44 eV and −5.67 eV, respectively.[7] In addition to this, the photocatalyst should possess a band gap between 1.5 and 3.0 eV in order to utilize UV light and visible light.[8,9]

Recently, various two-dimensional (2D) materials have been predicted to have remarkable photocatalytic activities.[10–12] First-principles calculations have predicted that single-layer group-III monochalcogenides are suitable for photocatalytic water splitting.[13] Some previous works demonstrated that single-layer MoS_2, WS_2, PtS_2 and $PtSe_2$ are potential photocatalysts due to their suitable band edges with respect to the redox potentials of water.[14–16] 2D SnS and GeSe materials are demonstrated to be promising alternative materials for optoelectronic applications.[17–20] Furthermore, heterobilayer GeSe/SnS could have promising applications in photovoltaic devices by modifying its electronic structure.[21] These 2D materials maximize the surface area available for water splitting and minimize the distance of generated electron and hole migration, which enhances their catalytic performance.[22]

Beyond 2D chalcogenide materials, metal halide materials with layered crystal structures (*e.g.*, PbI_2 and CdI_2) have also attracted significant attention due to their importance as precursors for the synthesis of halide perovskites.[23–27] Our previous works have demonstrated that layered PbI_2 possesses great potential in photovoltaic devices.[28,29] 2D CdI_2 nanoplates have also been synthesized by using a vapor transport and deposition approach.[25,30,31] However, the physical properties of 2D CdI_2 are far from clear. In particular, we focus on layered CdI_2 as a possible photocatalyst and propose some effective approaches to improve its photocatalytic performance.

Computational methods

All calculations are implemented in the VASP code[32,33] within the projector-augmented plane-wave method.[34] The generalized gradient approximation (GGA) of the Perdew, Burke and Ernzerhof (PBE) functional[35] is adopted for the electron exchange and correlation. The plane-wave cutoff energy is set as 450 eV and the HSE06 hybrid functional[36–38] is used to calculate the band structure of monolayer CdI_2. A vacuum larger than 15 Å is used to simulate the isolated sheet. The pair-wise force field in the DFT-D2 method of Grimme[39] is employed in the

School of Materials and Energy, Guangdong University of Technology, Guangzhou, Guangdong 510006, China. E-mail: huangle@semi.ac.cn

† Electronic supplementary information (ESI) available. See DOI: 10.1039/c7ra09687a

calculations of multilayer CdI_2 to correctly describe the vdW interactions between layers. For the relaxation of CdI_2 of various thicknesses, a (15 × 15 × 1) Monkhorst–Pack grid[40] is used, whereas for the relaxation of a doped CdI_2 monolayer, the first Brillouin zone is sampled with a (5 × 5 × 1) Monkhorst–Pack grid. All structures are fully relaxed with a force tolerance of 0.02 eV $Å^{-1}$.

Results and discussion

Compared with layered transition metal dichalcogenides, CdI_2 has a layered structure with a hexagonal unit cell and it crystallizes in the space group $P6_3mc$. This indicates that the 1T phase of CdI_2 is the most stable, rather than the 2H phase. As shown in Fig. 1a, each sheet of Cd atoms is sandwiched between two sheets of I atoms through strong ionic bonding,[41,42] and the atomic layers combined together *via* weak van der Waals (vdW) interactions. The optimized lattice constant of monolayer CdI_2 is 4.33 Å. Its band structure calculated on the PBE level indicates an indirect band gap of 2.53 eV in Fig. 1b. According to the calculated density of states (Fig. 1c), the VBM is mainly contributed to by Cd_p and I_p orbitals and the CBM is composed of I_p and Cd_s orbitals. In order to correct the PBE band gaps, a hybrid Heyd–Scuseria–Ernzerhof functional is adopted to describe the electron exchange and correlation (Fig. S1†). The general features of the band structure are well preserved except for a larger band gap than that of the PBE functional. Furthermore, the spin–orbit coupling (SOC) effect is taken into consideration in Fig. S1.† An obvious spin–orbit splitting is observed at the VBM of the band structure. As a result, the initial quadruple degenerate VBM becomes doubly degenerate. Meanwhile, the SOC exerts little influence on the CBM of the CdI_2 bands. This is attributed to the strong coupling between the Cd_d and I_p orbitals at the VBM and the absence of the Cd_d orbital at the CBM in the band structure of CdI_2. Although an indirect band gap is not favourable for water splitting, layered CdI_2 has suitable band edges to straddle the redox potentials of water. The photocatalytic activity can be enhanced when combining CdI_2 with other photocatalysts, such as C_3N_4, to construct a direct *Z*-scheme type photocatalysis system for water splitting.[43,44] What is more, the imaginary part of the dielectric function and light absorption (Fig. S2†) indicate good absorption in solar light. Our results are in good agreement with previous works except for an energy shift that is due to the underestimation of the GGA-PBE functional. CdI_2 thin films are reported by experimental works to have a direct optical energy gap of ~3.5 eV which seems too large for photocatalysis.[30,31] It is indicated by our results and previous experimental works that CdI_2 exhibits good absorption in ultraviolet light and has great potential in photocatalysis. Efficient ways to modulate its band edges are desired to improve the optoelectronic properties and the photocatalytic activity.

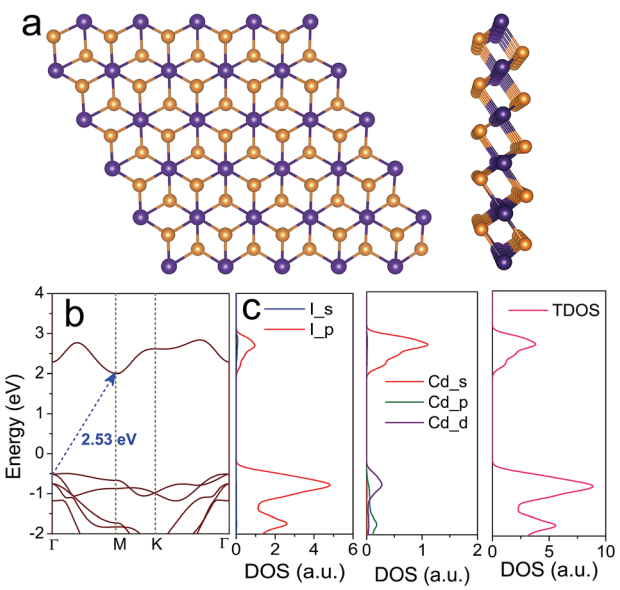

Fig. 1 (a) The lattice structure of single-layer CdI_2 from top and side views. The purple and brown balls denote the Cd and I atoms, respectively. (b) The band structure of single-layer CdI_2 and (c) the projected density of states (PDOS) and total density of states (TDOS).

It seems that the band gap of monolayer CdI_2 is too large to efficiently utilize the visible light in photocatalysis. It is well known that the electronic properties including the band gaps of most layered transition metal dichalcogenides are strongly dependent on the thickness of the materials.[45,46] Thus we checked the thickness-dependent electronic structure of CdI_2 as shown in Fig. 2a and b. It is indicated that both the CBM and the VBM approach the Fermi level, resulting in a decrease of the band gap of CdI_2 with thickness. The vacuum level is taken as a reference in Fig. 2b. It is indicated in Fig. 2b that the energies of both the CBM and the VBM increase with the number of layers. Furthermore, the band gap decreases gradually with the number of layers. The evolution of the band edges and band gap with the thickness is not very significant because of the rather weak interlayer coupling. What is more, the redox potentials of water are straddled between the band edges of CdI_2 with various thicknesses. The reduced band gap can make CdI_2 a good photocatalyst with it absorbing solar light over a wider wavelength range. Consequently, the photocatalytic performance can be improved to some extent by increasing the thickness of CdI_2 to a suitable value.

According to Fig. 2a and b, the band edges and band gap of CdI_2 exhibit weak dependence on the thickness with respect to most 2D transition metal dichalcogenides. An efficient approach to improve its photocatalytic performance is desired. It has been demonstrated that 2D materials exhibit significant modulation of their electronic structures by applying a normal strain. The evolution of the band structures of bilayer Cd_2 with an applied normal strain is shown in Fig. S3.† The normal strain is calculated as $\varepsilon = (d_0 - d)/d_0$. Our results indicate that the band gap of bilayer CdI_2 decreases with the applied normal strain (Fig. 2c). Clear insight can be obtained from the variation of the band edges of bilayer CdI_2 with the applied normal strain (Fig. 2d). The VBM increases gradually with the applied strain while the CBM does not show a monotonous trend because of the CBM's shift from the *M* point to the *Γ* point. Furthermore, the redox potentials of water are always straddled between the

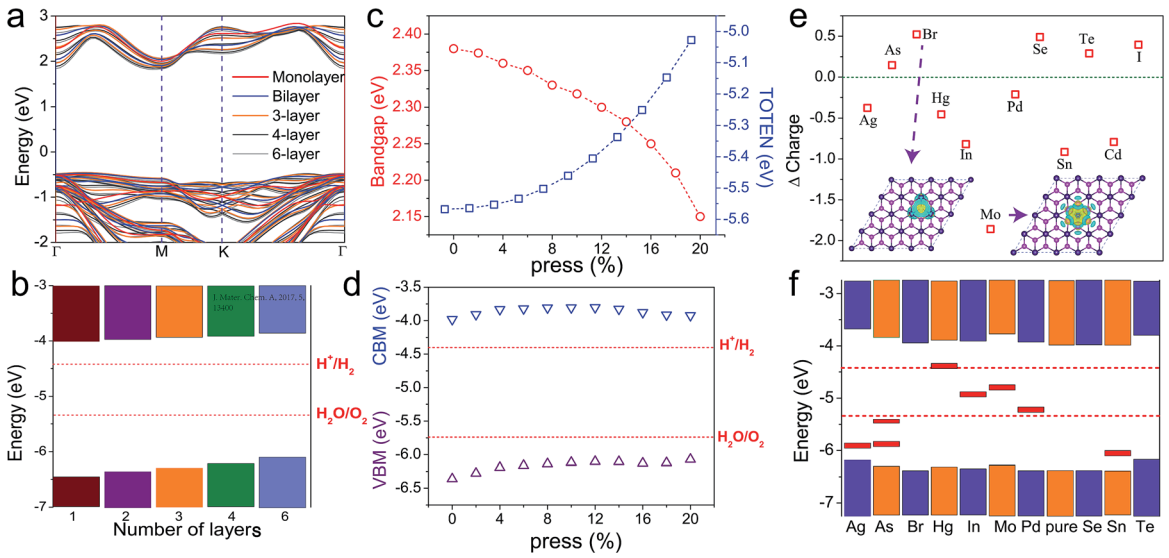

Fig. 2 (a) Band structures and (b) band alignments of CdI_2 of different thickness. Evolution of (c) band gap (red circles), total energy (blue squares) and (d) band edges of the CdI_2 bilayer as functions of the applied normal strain. (e) Transfer charge results from Bader charge analysis in the doped CdI_2 monolayer. The insets are the charge density difference in the Mo-doped and the Br-doped CdI_2 monolayer. (f) Band alignments of the doped CdI_2 monolayer. The red stripes in the band gap are the dopant bands introduced by substitution. The vacuum level is set as zero and is taken as a reference in (b), (d), and (f). The redox potentials of water are plotted as red dashed lines.

VBM and the CBM of the pressed CdI_2 bilayer. The CdI_2 bilayer with a reduced band gap from the application of normal strain is a good photocatalyst with improved performance due to the widened wavelength range for light absorption.

It should be mentioned that the interlayer binding in the CdI_2 bilayer is relatively weaker than that in most of the transition metal dichalcogenide bilayers such as those of MoS_2. Fig. 2c also shows the evolution of the total energy of the CdI_2 bilayer. The charge density difference (Fig. S4†) shows slight charge transfer between layers in the CdI_2 bilayer upon binding together. The weak binding gives rise to the relatively weak response of the electronic structure and strain energy to the applied strain. Similar evidence comes from the integrated charge density of the CdI_2 bilayer under different normal strain (Fig. S5†). It is found that applying a normal strain will bring about extra charge exchanging between layers. It can be concluded that applying a normal strain is an efficient way to improve the photocatalytic performance.

Besides applying normal strain, substituted doping has also been demonstrated to be an effective method to modulate the band alignment of a semiconductor. In Fig. 2e and f, several non-magnetic atoms are employed to make substituting dopants in a $(4 \times 4 \times 1)$ CdI_2 monolayer supercell. Dopant bands are induced either in the band gap or near the band edges (Fig. S6†), which should exert a significant influence on the optoelectronic and photovoltaic properties of monolayer CdI_2. In Fig. 2e, Bader charge analysis demonstrates that charge transfer occurs between dopants and it defected the CdI_2 monolayer.

The band alignments of these doped CdI_2 monolayers are plotted in Fig. 2f. It is found that In, Mo and Pd will introduce dopant bands in the redox potential of water, making the corresponding doped CdI_2 not suitable for photocatalysis, while other dopants employed here will not introduce extra bands in the redox potential of water. Ag, As and Sn dopants will induce extra bands between the VBM and the H_2O/O_2 potential, and Hg can induce extra bands between the H^+/H_2 potential and the CBM, making the corresponding doped CdI_2 suitable for photocatalysis in water splitting.

In many optoelectronic and photovoltaic devices, the materials are always subjected to a vertical electric field ($E_\perp$). Multilayer 2D materials usually exhibit significant modulation of their electronic structures by applying an $E_\perp$. As shown in Fig. 3a, the band structures of the CdI_2 bilayer under different $E_\perp$ are calculated. Our results indicate that its band gap is significantly reduced by the applied $E_\perp$. Further insight can be obtained from the variation of the band edges with the $E_\perp$ in Fig. 3b. It is clear that the CBM exhibits a linear descending trend with the $E_\perp$ while the VBM is hardly influenced by the $E_\perp$. As a photocatalyst, when subjected to a vertical electric field, the CBM of CdI_2 will approach the H^+/H_2 level. This will improve the absorption of solar light, further leading to enhanced photocatalytic activity. However, a strong $E_\perp$ will reduce the CBM of CdI_2 to the position below the H^+/H_2 level, making CdI_2 unsuitable as a photocatalyst.

To make the distinct responses of the VBM and the CBM to the applied $E_\perp$ clear, the band decomposed charge density of the CBM and the VBM at the four high-symmetry k-points (Γ, M, K, A) is shown in Fig. 3c and d. A is the k-point between K and Γ, which is given in Fig. 3a. As can be seen, the lowest-energy carriers (holes) are almost completely localized around the I atoms, forming π bonds. The absence of a polarized distribution between the I and Cd atoms results in the weak response of the VBM to the applied $E_\perp$, while at the CBM, the lowest-energy

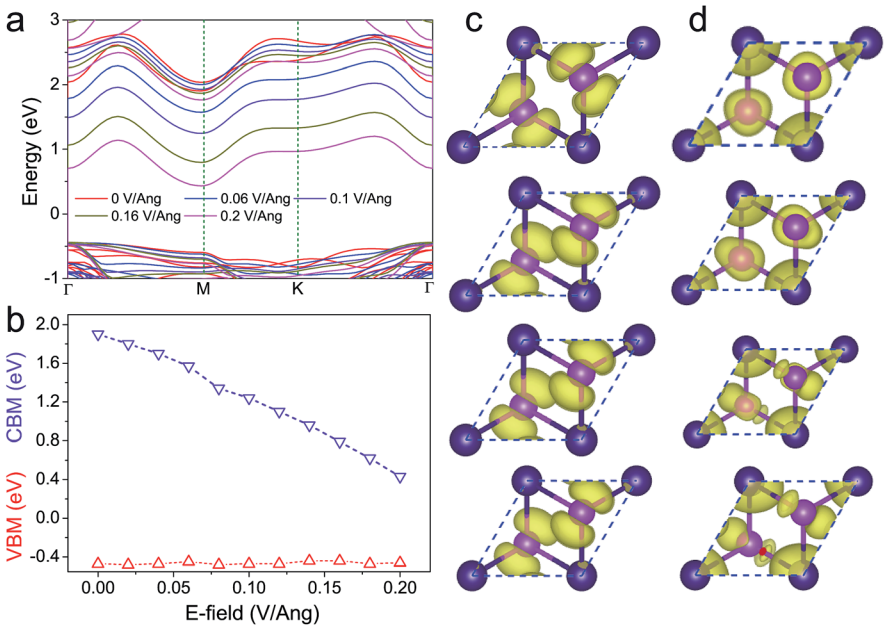

Fig. 3 Evolution of the (a) band structure and (b) band edges of the CdI_2 bilayer as functions of the applied vertical electric field. (c) and (d) plot the band decomposed charge density of the VBM and CBM at four high-symmetry k-points (Γ, *M*, *K*, *A*) of the CdI_2 bilayer, respectively. The *A* point is the *k*-point between the *K* and the Γ points.

carriers (electrons) are neither localized on the I atoms nor the Cd atoms. Charge exchange exists between I and Cd atoms. As a result, the applied $E_\perp$ exerts a significant influence on the CBM.

Conclusions

In summary, the electronic structure of 2D CdI_2 is explored by density functional theory calculations. The calculated results of the band gaps and band edges demonstrated that CdI_2 is a suitable photocatalyst for water splitting. Monolayer CdI_2 should exhibit a low photocatalytic activity due to its large band gap (about 3.0 eV). Multilayer CdI_2 with a narrower band gap may absorb a finite amount of visible light, making it a more suitable photocatalyst. What is more, its photocatalytic activity can be enhanced by applying normal strain and a vertical electric field with two distinct mechanisms. Both the CBM and VBM of bilayer CdI_2 can be tuned by applying a normal strain, while a vertical $E_\perp$ is only able to modulate the CBM of bilayer CdI_2. Some favourable substituting dopants can also make the band alignment of CdI_2 more suitable for photocatalysis. These results provide valuable guidance for enhancing the photocatalytic activity of 2D CdI_2.

Conflicts of interest

There are no conflicts to declare.

Acknowledgements

This work was financially supported by the National Natural Science Foundation of China (Grant no. 11674310, 61622406, 61571415, 51502283, and 51602065), the National Key Research and Development Program of China (Grant No. 2016YFB0700700), "Hundred Talents Program" of Chinese Academy of Sciences (CAS), and the CAS/SAFEA International Partnership Program for Creative Research Teams.

References

1 T. Simon, N. Bouchonville, M. J. Berr, A. Vaneski, A. Adrovic, D. Volbers, R. Wyrwich, M. Döblinger, A. S. Susha, A. L. Rogach, *et al.*, *Nat. Mater.*, 2014, **13**, 1013.
2 X. Chen, L. Liu, Y. Y. Peter and S. S. Mao, *Science*, 2011, **331**, 746.
3 R. Asahi, T. Morikawa, H. Irie and T. Ohwaki, *Chem. Rev.*, 2014, **114**, 9824.
4 J. Ran, J. Zhang, J. Yu, M. Jaroniec and S. Z. Qiao, *Chem. Soc. Rev.*, 2014, **43**, 7787.
5 Y. Gai, J. Li, S.-S. Li, J.-B. Xia and S.-H. Wei, *Phys. Rev. Lett.*, 2009, **102**, 036402.
6 J. Kang, S. Tongay, J. Zhou, J. Li and J. Wu, *Appl. Phys. Lett.*, 2013, **102**, 012111.
7 V. Chakrapani, J. C. Angus, A. B. Anderson, S. D. Wolter, B. R. Stoner and G. U. Sumanasekera, *Science*, 2007, **318**, 1424.
8 A. K. Singh, K. Mathew, H. L. Zhuang and R. G. Hennig, *J. Phys. Chem. Lett.*, 2015, **6**, 1087.
9 S. Chen and L.-W. Wang, *Chem. Mater.*, 2012, **24**, 3659.
10 W. J. Ong, *Front. Mater.*, 2017, **4**, 11.
11 D. Zeng, L. Xiao, W. J. Ong, P. Wu, H. Zheng, Y. Chen and D. L. Peng, *J. Mater. Chem. A*, 2017, **5**, 16171–16178.
12 X. Lv, W. Wei, Q. Sun, F. Li, B. Huang and Y. Dai, *Appl. Catal., B*, 2017, **217**, 275.

13 H. L. Zhuang and R. G. Hennig, *Chem. Mater.*, 2013, **25**, 3232.
14 H. L. Zhuang and R. G. Hennig, *J. Phys. Chem. C*, 2013, **117**, 20440.
15 N. Singh, G. Jabbour and U. Schwingenschlögl, *Eur. Phys. J. B*, 2012, **85**, 392.
16 G. Guo and W. Liang, *J. Phys. C: Solid State Phys.*, 1986, **19**, 995.
17 P. D. Antunez, J. J. Buckley and R. L. Brutchey, *Nanoscale*, 2011, **3**, 2399.
18 A. K. Singh and R. G. Hennig, *Appl. Phys. Lett.*, 2014, **105**, 042103.
19 Z. Ma, B. Wang, L. Ou, Y. Zhang, X. Zhang and Z. Zhou, *Nanotechnology*, 2016, **27**, 415203.
20 L. Huang, F. Wu and J. Li, *J. Chem. Phys.*, 2016, **144**, 114708.
21 C. Xia, J. Du, W. Xiong, Y. Jia, Z. Wei and J. Li, *J. Mater. Chem. A*, 2017, **5**, 13400.
22 A. Kudo and Y. Miseki, *Chem. Soc. Rev.*, 2009, **38**, 253.
23 Y. Hu, Y. Guo, Y. Wang, Z. Chen, X. Sun, J. Feng, T. M. Lu, E. Wertz and J. Shi, *J. Mater. Res.*, 2017, **325**, 1.
24 J. Zhang, T. Song, Z. Zhang, K. Ding, F. Huang and B. Sun, *J. Mater. Chem. C*, 2015, **3**, 4402.
25 R. Ai, X. Guan, J. Li, K. Yao, P. Chen, Z. Zhang, X. Duan and X. Duan, *ACS Nano*, 2017, **11**, 3413.
26 I. Karbovnyk, I. Bolesta, I. Rovetskyi, V. Lesivtsiv, Y. Shmygelsky, S. Velgosh and A. Popov, *Low Temp. Phys.*, 2016, **42**, 594.
27 J. Robertson, *J. Phys. C: Solid State Phys.*, 1979, **12**, 4753.
28 M. Zhong, S. Zhang, L. Huang, J. You, Z. Wei, X. Liu and J. Li, *Nanoscale*, 2017, **9**, 3736.
29 M. Zhong, L. Huang, H.-X. Deng, X. Wang, B. Li, Z. Wei and J. Li, *J. Mater. Chem. C*, 2016, **4**, 6492.
30 P. Tyagi, A. G. Vedeshwar and N. C. Mehra, *Phys. B*, 2001, **304**, 166.
31 I. A. Kariper, *J. Mater. Res. Technol.*, 2016, **5**, 77.
32 G. Kresse and J. Furthmüller, *Phys. Rev. B*, 1996, **54**, 11169.
33 G. Kresse and J. Furthmüller, *Comput. Mater. Sci.*, 1996, **6**, 15.
34 P. E. Blöchl, *Phys. Rev. B*, 1994, **50**, 17953.
35 J. P. Perdew, K. Burke and M. Ernzerhof, *Phys. Rev. Lett.*, 1996, **77**, 3865.
36 J. Heyd, G. E. Scuseria and M. Ernzerhof, *J. Chem. Phys.*, 2003, **118**, 8207.
37 J. Heyd, J. E. Peralta, G. E. Scuseria and R. L. Martin, *J. Chem. Phys.*, 2005, **123**, 174101.
38 J. Heyd, G. E. Scuseria and M. Ernzerhof, *J. Chem. Phys.*, 2006, **124**, 9906.
39 S. Grimme, *J. Comput. Chem.*, 2006, **27**, 1787.
40 H. J. Monkhorst and J. D. Pack, *Phys. Rev. B*, 1976, **13**, 5188.
41 İ. A. Kariper, *J. Mater. Res. Technol.*, 2016, **5**, 77.
42 Y. Wang, Y.-Y. Sun, S. Zhang, T.-M. Lu and J. Shi, *Appl. Phys. Lett.*, 2016, **108**, 013105.
43 J. Wang, Z. Guan, J. Huang, Q. Li and J. Yang, *J. Mater. Chem. A*, 2014, **2**, 7960.
44 Q. Li, N. Zhang, Y. Yang, G. Wang and D. H. Ng, *Langmuir*, 2014, **30**, 8965.
45 W. Jin, P.-C. Yeh, N. Zaki, D. Zhang, J. T. Sadowski, A. Al-Mahboob, A. M. van Der Zande, D. A. Chenet, J. I. Dadap, I. P. Herman, *et al.*, *Phys. Rev. Lett.*, 2013, **111**, 106801.
46 R. Coehoorn, C. Haas, J. Dijkstra, C. Flipse, R. De Groot and A. Wold, *Phys. Rev. B*, 1987, **35**, 6195.